

Dendrimer pre-treatment enhances the skin permeation of chlorhexidine digluconate: characterisation by in vitro percutaneous absorption studies and time-of-flight secondary ion mass spectrometry

Amy M. Holmes*, David J. Scurr, Jon R. Heylings, Ka-Wai Wan & Gary P. Moss*

A. M. Holmes* G. P. Moss*

School of Pharmacy, Keele University, Keele
Staffordshire ST5 5BG, UK

A. M. Holmes (current)

School of Pharmacy and Medical sciences
University of South Australia, Adelaide, South Australia, 5000

D. J. Scurr

School of Pharmacy, University of Nottingham, Nottingham, UK

J. R. Heylings

Dermal Technology Laboratory Ltd.

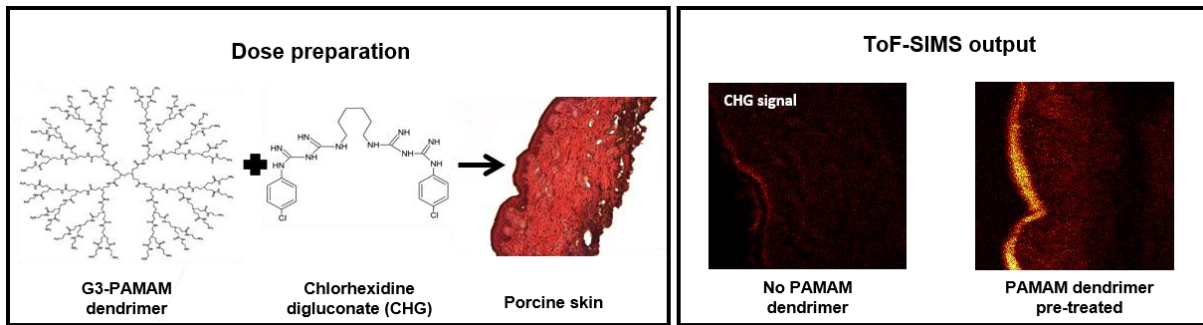
MedIC4, Keele University Science and Innovation Park,
Keele, Staffordshire, ST5 5NL, UK

K.-W. Wan

School of Pharmacy and Biomedical Sciences
University of Central Lancashire, Preston, UK

*corresponding authors (amy.holmes@unisa.edu.au; g.p.j.moss@keele.ac.uk)

Graphical abstract



Key Words

PAMAM dendrimer

Time-of-Flight Secondary Ion Mass Spectrometry

Chlorhexidine

In vitro skin diffusion

Tape stripping

Penetration Enhancer

Acknowledgements and disclosures

This work was funded by an EPSRC industrial CASE award in collaboration with Dermal Technology Laboratory Ltd. The authors would like to acknowledge Professor Steve Chapman for his assistance and David Griffiths for his help and advice with the skin cryo-sectioning and histology. The authors state no conflict of interest.

Abstract

Skin penetration and localisation of chlorhexidine digluconate (CHG) within the skin have been investigated in order to better understand and optimise the delivery using a nano polymeric delivery system of this topically-applied antimicrobial drug. Franz-type diffusion cell studies using *in vitro* porcine skin and tape stripping procedures were coupled with Time-of-Flight Secondary Ion Mass Spectrometry (ToF-SIMS) to visualise the skin during various treatments with CHG and polyamidoamine dendrimers (PAMAM). Pre-treatment of the skin with PAMAM dendrimers significantly increased the amount and depth of permeation of CHG into the skin *in vitro*. The effect observed was not concentration dependant in the range 0.5 – 10 mM PAMAM. This could be important in terms of the efficiency of treatment of bacterial infection in the skin. It appears that the mechanism of enhancement is due to the PAMAM dendrimer disrupting skin barrier lipid conformation or by occluding the skin surface. Franz-type diffusion cell experiments are complimented by the detailed visualisation offered by the semi-quantitative ToF-SIMS method which provides excellent benefits in terms of sensitivity and fragment ion specificity. This allows a more accurate depth profile of chlorhexidine permeation within the skin to be obtained and potentially affords the opportunity to map the co-localisation of permeants with skin structures, thus providing a greater ability to characterise skin absorption and to understand the mechanism of permeation, providing opportunities for new and more effective therapies.

INTRODUCTION

Chlorhexidine (1,6-di(4-chlorophenyl-diguanido)hexane) (CHG) is a cationic bisbiguanide. It has a broad spectrum of antimicrobial activity and a low toxicity to mammalian cells [1]. It has been used extensively for the last sixty years in a range of formulations including water, ethanol and isopropyl alcohol based preparations. It has been used extensively in a range of topical formulations; however, its skin permeability has been shown to be poor. For example, while it was demonstrated that permeability from aqueous solutions was time-dependant, its overall permeation was limited, with the permeant accumulating mostly in superficial tissues of the skin and with no penetration across full-thickness skin being observed [2]. Similar results for permeation of CHG into and across rodent skin were reported elsewhere [3]. Such studies clearly indicate that the poor skin permeability of CHG, ostensibly due to its physicochemical properties (i.e. molecular weight of 897.8) and may allow potential pathogens to remain viable within deeper layers of the skin.

One of the broader limitations of such studies, not just those confined to CHG, but to all potential percutaneous penetrants, is the analytical methodology employed to discern absorption into and across skin tissues. Tape stripping methods are limited by a lack of method standardisation, incomplete removal of the *stratum corneum* and inconsistent removal of skin layers [4,5]. While a number of studies [6 – 8] have suggested iterations to tape stripping methodology to alleviate such issues, it is a method that does not permit identification of the histological compartments within skin in which a permeant might reside. This extends to location of the compound of interest with the dermis or epidermis as the tape strips may overlap both of those regions. Furthermore, horizontal sectioning is a time-consuming and laborious process.

Deposition and distribution of CHG on, and within, skin was recently characterised for the first time by Time-of-Flight Secondary Ion Mass Spectrometry (ToF-SIMS) [9]. ToF-SIMS imaging analysis involves the rastering of a pulsed primary ion beam over a surface of the tissue samples, leading to a collision cascade and the production of secondary ions [10]. Chemical maps of selected secondary ions can be retrospectively constructed for the area analysed [11]. ToF-SIMS analysis provides excellent sensitivity to the ppm range, including the parallel detection of isotopes and spatial localisation of permeants within tissue structures. The ToF-SIMS method therefore obviates the need for complex sample preparation or the use of radiolabelling. It therefore allows the distribution of a compound within a biological tissue to be mapped and may even yield information on the mechanisms underpinning such permeability and skin localisation. ToF-SIMS has been applied to analyse the skin

by a number of researchers to explore the effects of photo ageing on human skin and to characterise the distribution of synthetic pseudoceramides delivered from a cosmetic formulation [12 – 14]. Most recently, this method has been applied to the characterisation of age-related changes to human *stratum corneum* lipids following *in vivo* sampling, which identified alterations to the spatial distribution of a number of *stratum corneum* lipids associated with membrane stability [15].

Classical *in vitro* Franz cell permeation studies have previously been combined with the ToF-SIMS analysis of skin. This combination of methods was used to characterise the distribution of CHG delivered from simple vehicles into skin, including the benchmarking of tape strips against the ToF-SIMS method, where it was found that the ToF-SIMS method has a lower limit of detection than the tape stripping methods [9].

A more comprehensive characterisation of CHG skin permeability was reported recently [16]. The authors presented both high mass resolution mass spectra and high spatial resolution images provided by ToF-SIMS from cryosectioned samples that followed a 24-hour application of CHG (2% w/w solution) to porcine skin in a Franz-type diffusion cell model. CHG distribution was mapped throughout the skin sections and confirmed that it was predominately localised within the *stratum corneum*. This was compared to ToF-SIMS analysis of tape strips which supported the distribution profile within the skin tissue. Thus, the ToF-SIMS methods demonstrated excellent complementarity to diffusion cell experiments and the ability to image samples with high chemical specificity without the need for radiolabels. The ToF-SIMS data allows for the visualisation of the drug deposition on each corneocyte layer of individual tape strips so that detailed permeation profiles of a drug throughout the *stratum corneum* can be obtained.

Poly(amidoamine) (PAMAM) dendrimers have previously been used as percutaneous absorption enhancers for a number of topically applied therapeutics where they have demonstrated the ability to conjugate to drugs bound to their surface or to encapsulate drugs within their structure [17 - 22]. The properties exhibited by PAMAM dendrimers have allowed for the protection of degradable drugs, increased the aqueous solubility of drugs and have been shown to ameliorate modified drug release through thermo- or pH-responsive properties [23 – 25].

PAMAM dendrimers have also demonstrated the ability to act as transdermal drug carriers by facilitating skin permeation of 5-fluorouracil into porcine skin [26]. The G4-PAMAM-OH and G4-PAMAM-NH₂ dendrimers have been shown to enhance the permeation of indomethacin across skin *in*

vitro by a factor of 4.5, where the dendrimer formed a complex with indomethacin through electrostatic and hydrophobic bonding [27]. However, G4-PAMAM-NH₂ dendrimers generally have a greater *in vivo* toxicity than the lower generation (G0-G2) PAMAMs i.e. smaller dendrimers with a lower molecular weight and fewer surface functionalities, limiting significantly their clinical applications.

The aim of this present study is to evaluate the role of PAMAM dendrimers as enhancers of chlorhexidine permeation into and across porcine skin. As well as conventional Franz-type diffusion cell studies, including tape stripping of the *stratum corneum*, ToF-SIMS analysis of cryosectioned skin sections was performed to visualise the permeation and distribution of CHG within the skin.

METHODS

Materials

The G3-PAMAM-NH₂ dendrimer (Sigma Aldrich product code 412422, molecular weight 6909 Da, supplied in methanol for reasons of stability and diluted in water prior to use), chlorhexidine digluconate, sodium chloride, sodium octane-1-sulphonate, triethylamine, glacial acetic acid and optimal cutting temperature media were purchased from Sigma Aldrich (Dorset, UK). HPLC grade methanol and syringe filters 0.2 µm, 15 mm diameter polypropylene filters were purchased from Fisher Scientific, Loughborough, UK). The MetLab ODS-H reverse phase column (150 × 4.6 mm, 5 µm) and HPLC vials were purchased from Phenomenex (Cheshire, UK).

In vitro percutaneous absorption in a porcine skin model

Method overview

Two types of skin preparation were used in this investigation. Epidermal membranes were prepared from whole pig ears by heat separation to study the absorption of CHG into the receptor fluid following PAMAM pre-treatment. In order to study the localisation of CHG in the different regions of the skin, using a tape stripping technique, whole pig skin samples from the flank were dermatomed to produce 400µm split thickness samples, prior to mounting them in the Franz diffusion cells. Both methods of skin preparation are

permitted in OECD test guideline 428 for the assessment of dermal absorption *in vitro*. Thus, all investigations of percutaneous absorption using Franz-type diffusion cells described in this study were conducted according to the OECD method as discussed in detail elsewhere [9, 16]. Pig ears were obtained as a residue of food production (but not subject to steam cleaning), they were shaved, gently cleaned and the subcutaneous fat and cartilage was removed. The skin was prepared by heat separation and placed in Franz static diffusion cells. Skin barrier integrity was determined to be intact by measurement of transepithelial electrical resistance (TEER). An electrical resistance reading of ≥ 3 K Ω has been previously shown to represent the normal barrier integrity of pig ear skin in the static diffusion cells used in this investigation [28 – 31].

The effect of PAMAM dendrimer pre-treatment on the in vitro permeation on CHG using porcine epidermis

Physiological saline was used as the receptor phase in diffusion experiments as it provided adequate sink conditions for the penetrant. Briefly, 4.5 mL of physiological saline was added to the receptor chamber of each Franz cell. The Franz cells (n = 15 – 24; see Table 2) were placed in the water bath (32°C \pm 1°C) on a submersible stirring plate for 30 minutes and allowed to equilibrate. Both a G3-PAMAM-NH₂ (0.5 mM-10 mM, diluted in MilliQ water) and a 2% (w/v) solution of CHG were prepared in distilled water from stock solutions of G3-PAMAM-NH₂ (20% (w/v)) and CHG (20% (w/v)) respectively. 0.2 mL of G3-PAMAM-NH₂ (0.5 mM-10 mM) was then applied to the skin surface for a 24 h contact time. The vehicle was dosed without the presence of PAMAM dendrimer in the cells representing the controls. At the end of the exposure period, the PAMAM dendrimer was then washed from the skin surface by rinsing with 2 mL aliquots of distilled water (10 mL in total) pipetted over the surface of the dosed skin, taking care not to damage the skin surface. An infinite dose (1 mL) of the CHG solution (2% w/v) was then applied to the skin surface and left for a contact time of 24 h. At various time points during this 24 h period a 500 μ L aliquot of receptor fluid was removed and replaced with fresh physiological saline. After 24 h, excess CHG was removed from the skin surface by further

washing. The skin sample was then removed from the diffusion chamber and the skin prepared for CHG extraction and subsequent HPLC analysis as described previously [16].

Franz diffusion cell studies using porcine dermatomed skin for tape stripping.

Additional Franz cells were dosed as described in the preceding section but the skin was also tape-stripped at the end of the experiment using the gravimetric method reported previously [32] with a four-figure balance (Precisa, 262 SMA-FR, Milton Keynes, UK). Once 21 tape strips had been taken they were pooled together; tape strips 1-3 were analysed as individual tape strips. Tape strips 4-6, 7-10, 11-16 and strips 17-21 were pooled together and CHG was extracted in 10 mL of HPLC mobile phase. The remaining tape stripped skin and the glass donor chambers were also extracted overnight in 10 mL of HPLC mobile phase. The receptor fluid time point aliquots were prepared for analysis by syringe filtering and vortex mixing and, if appropriate, dilution [8]. Normalisation of the drug content on tapes strips was conducted by using the method described in work by Reddy *et al* using [33]:

$$C_n = \frac{m_n \cdot \rho_{sc}}{m_{sc,n}} \quad (1)$$

where C_n is the concentration of the drug of the n^{th} tape strip accounting for the mass of *stratum corneum* material, which has been determined gravimetrically;
 m_n is the mass of drug in the n^{th} tape strip
 ρ_{sc} is the density of the *stratum corneum*, assumed to be 1g/cm^3 [34]
 $m_{sc,n}$ is the mass of *stratum corneum* on the tape strip, determined gravimetrically

HPLC Analysis of CHG

HPLC analysis of CHG samples was adapted from the method detailed in work by Karpanen *et al.* [2]. Analysis was conducted on a Shimadzu UCFC Modula system with an SPD M20 diode array detector using an isocratic mobile phase consisting of a methanol: water mixture (75:25) with 0.005 M sodium octane-1-sulphonate and 0.1% (v/v) triethylamine. The pH was adjusted with glacial acetic acid to pH

4. The flow rate was 1.5 mL per minute on a MetLab ODS-H reverse phase column (150 × 4.6 mm, 5 µm) that was set for 40 °C. Mobile phase was used as the solvent for all CHG extractions [2]. The limit of detection (LOD) and limit of quantification (LOQ) were determined to be 0.050 µg/mL and 0.167 µg/mL, respectively. The relative standard deviation (RSD) was calculated for 6 repeats of the 10 µg/mL standard and was found to be 0.40%. For the skin assays conducted in this study the %RSD for each standard was <5% and R² was 0.9999.

Statistical analysis

All data is presented as the mean ± standard error of the mean (SEM), unless otherwise stated. Analysis was conducted via GraphPad Prism® version 5 (San Diego, USA). Prior to statistical analysis all data were checked for normality using the D'Agostino-Pearson test running on GraphPad Prism software. To compare the mean total concentration of CHG detected within the porcine epidermis after the various skin pre-treatments described above a Kruskal-Wallis ANOVA test was conducted as the data was non-parametric, with $p < 0.05$ representing significance. A Kruskal-Wallis ANOVA with a Dunn's post-test to compare treatment groups was also performed to determine if there was a difference in total CHG concentrations within the receptor fluid at 24 h for the different skin pre-treatment groups. A Kruskal-Wallis ANOVA test was used to determine whether there was a significant difference between the total CHG concentration extracted from the tape strips after various skin pre-treatments with $p < 0.05$ signifying statistical significance. Furthermore, a Kruskal-Wallis test with a Dunn's post-test was also employed to determine whether there was a significant difference in CHG concentration within the epidermis and dermis after various skin pre-treatments.

Time-of-Flight Secondary Ion Mass Spectrometry analysis of skin samples

Sample preparation for ToF-SIMS analysis

Prior to ToF-SIMS analysis, samples were prepared and analysed using the methods reported previously [9, 16]. Following the Franz cell experiments the skin samples were frozen at -80°C until required. The frozen skin samples were mounted on a cryostat using Optimal Cutting Temperature embedding material. Vertical cross sections of skin (8 µm) were cut and placed on to a clean glass cover-slip (1 cm × 1 cm); the cover slips were first rinsed in ultra-pure water followed by methanol, chloroform and finally hexane before the skin sample was loaded. The 21 tape strips taken from diffusion cell experiments were then freeze-dried and placed on a solvent-cleaned microscope slide ready for analysis.

ToF-SIMS analysis

Analysis was performed using a ToF-SIMS IV instrument (IONTOF, GmbH, Münster, Germany) employing a Bi₃⁺ primary ion source and a single-stage reflectron analyzer. Data acquisition and analysis was performed using SufaceLab 6 software. Both positive and negative spectra were acquired at a resolution of 256 × 256 pixels by scanning a primary beam over the sample area (500 × 500 µm). Charge compensation was performed by irradiation of the sample with a pulsed beam of electrons using an electron flood gun. Although data was collected in both positive and negative polarity, only the negative ion data are presented as the positive ion data, though supportive, was found to be much less informative. All CHG markers were chosen from spectra that were operated in the bunched mode [9, 16].

Statistical analysis of data

All data shown in the ToF-SIMS study is displayed as the mean ± either SEM or SD, as stated, followed by the sample number. To determine whether there was a statistical significance between the measured CHG ingress (µm) within the skin, with and without a PAMAM dendrimer pre-treatment, a two-way t-test was conducted via GraphPad Prism® version 5 (San Diego, USA) after confirming the data was normally distributed.

RESULTS

Recovery of CHG

CHG is known to adsorb onto a variety of surfaces including glass, cotton wool and skin [1]. Mass balance experiments were carried out in all studies in line with the expectations of OECD 428 [16, 9]. The % of recovered CHG from each Franz cell compartment was very similar across the three concentrations tested (Table 1) and the variance observed suggested that the adsorption of CHG onto the surfaces is not concentration dependent but more likely surface area dependent. The recovery in all experiments was within the expected range according to OECD 428 guidelines. The percentage of dosed CHG that was not recovered from the glass donor chamber was ~9%, but silanisation of the diffusion cells did not enhance the recovery of the dosed CHG.

Table 1. Percentage recovery of three concentrations of aqueous chlorhexidine digluconate (CHG) after spiking each Franz cell compartment with 100µl CHG (n=3).

CHG concentration	Percentage recovered dose spiked onto Franz cell compartments after 24 hours		
	Epidermis	Adhesive tape strip	Donor chamber
1% (w/v) CHG dosed	88	94	93
	84	92	91
	86	94	91
Mean ± SEM	86.00 ± 1.155	93.33 ± 0.067	91.67 ± 0.0667
5% (w/v) CHG dosed	88	91	91
	82	94	88
	81	91	93
Mean ± SEM	83.67 ± 2.186	92.00 ± 1.000	90.67 ± 1.453
10% (w/v) CHG dosed	84	92	88
	86	97	94
	84	94	91
Mean ± SEM	84.67 ± 0.667	94.33 ± 1.453	91.00 ± 1.732

The effect of PAMAM dendrimer pre-treatment on the in vitro permeation on CHG using porcine epidermis

Table 2 summarises the results from the pre-treatment skin absorption studies. It lists concentrations of CHG found in skin washes, donor chamber, epidermal tissue and the receptor fluid after the 24 h duration of the experiments. Table 2 also lists the rate of absorption (flux values) associated with each experiment. Results are shown for four experiments; pre-treatment as a control (with saline as the control) and 0.5, 1.0 and 10.0 mM solutions of the G3-PAMAM-NH₂ dendrimer.

Table 2. Compartmental diffusion cell data and rates of absorption over of CHG 24 h (0 - 12 h; 15 - 24 h and 0 - 24 h) after a skin pre-treatment of G3-PAMAM-NH₂ dendrimer (0.5 – 10.0 mM, plus control).

Sample	Control sample (no dendrimer pre-treatment) (n=15)				Pre-treatment (0.5 mM) (n=19)				Pre-treatment (1.0 mM) (n=24)				Pre-treatment (10 mM) (n=24)			
	CHG ($\mu\text{g}/\text{cm}^2$)		% of applied dose		CHG ($\mu\text{g}/\text{cm}^2$)		% of applied dose		CHG ($\mu\text{g}/\text{cm}^2$)		% of applied dose		CHG ($\mu\text{g}/\text{cm}^2$)		% of applied dose	
	Mean	SEM	Mean	SEM	Mean	SEM	Mean	SEM	Mean	SEM	Mean	SEM	Mean	SEM	Mean	SEM
Donor chamber	815.129	154.935	10.354	1.967	307.786	59.483	3.909	0.755	700.350	96.384	8.890	1.224	617.035	136.620	7.836	1.735
Skin wash	4080.063	398.892	51.817	5.066	4515.081	301.075	57.342	3.824	3924.292	291.115	49.839	3.697	4419.776	285.820	56.131	3.630
Epidermis	1030.668	130.917	13.089	1.662	1202.763	177.213	15.275	2.251	986.226	118.160	12.525	1.501	1421.675	187.069	18.055	2.376
Receptor fluid	3.226	1.622	0.041	0.020	92.013	34.490	1.169	0.438	47.324	12.150	0.601	0.154	82.912	16.681	1.053	0.212
Total recovered	5929.086	686.366	75.299	8.715	6117.643	572.261	77.694	7.268	5658.192	517.809	71.855	6.576	6541.388	626.19	83.075	7.953
	Control sample (no dendrimer pre-treatment) (n=15)				Pre-treatment (0.5 mM) (n=19)				Pre-treatment (1.0 mM) (n=24)				Pre-treatment (10 mM) (n=24)			
	Absorption rate ($\mu\text{g}/\text{cm}^2/\text{h}$)				Absorption rate ($\mu\text{g}/\text{cm}^2/\text{h}$)				Absorption rate ($\mu\text{g}/\text{cm}^2/\text{h}$)				Absorption rate ($\mu\text{g}/\text{cm}^2/\text{h}$)			
	0-12 h	15-24 h	0-24 h		0-12 h	15-24 h	0-24 h		0-12 h	15-24 h	0-24 h		0-12 h	15-24 h	0-24 h	
Mean	0.0164	0.219	0.097		0.395	1.618	0.890		0.174	1.100	0.612		0.477	1.525	0.980	
SEM	0.0126	0.103	0.045		0.254	0.402	0.221		0.063	0.250	0.139		0.137	0.318	0.193	

Table 2 shows that the majority of applied CHG (approximately 60%) remains on the skin surface or the donor compartment at the end of the experiment. Approximately 13 – 18% of the applied dose is found in the epidermis, including the superficial *stratum corneum*, with a very small amount, of approximately 0.04 – 1.20%, found in the receptor compartment of the diffusion cell. Flux was found to be biphasic in many cases and the absorption rates for 0 – 12 hours and 15 – 24 hours are listed in Table 2, along with the overall absorption rate for the 24 hour experiments.

The trends in CHG flux are summarised in Figure 1. In Figure 1 (a) the diffusion profiles clearly illustrate the biphasic release profiles and the distinction between the control pre-treatment experiment and the dendrimer pre-treatments (0.5, 1.0 and 10.0 mM). The concentration profiles for CHG were very similar across all PAMAM dendrimer concentrations tested up to a time period of 9 h. The largest concentration increase was observed in the 12-24 h time period. Figure 1 (b) shows the concentration of CHG extracted from the epidermis after 24 h for all four skin pre-treatments. Though the 10 mM G3-PAMAM-NH₂ dendrimer skin pre-treatment yielded the highest CHG deposition within the epidermis, no significant difference was observed between the CHG concentrations ($\mu\text{g}/\text{cm}^2$) extracted from the epidermis for the four skin pre-treatment groups (Kruskal Wallis ANOVA, $p>0.05$).

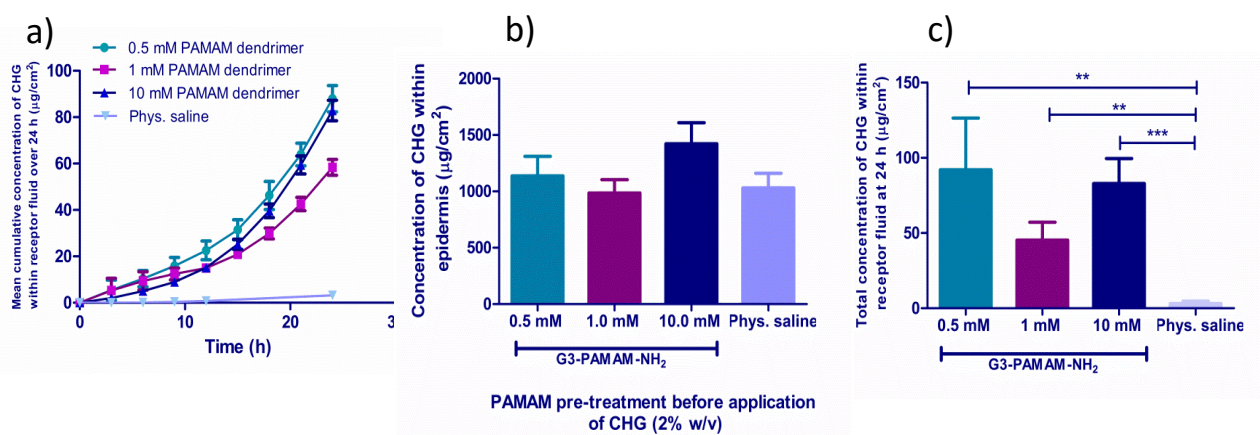


Figure 1. Results of diffusion cell studies for CHG: (a) concentration of CHG (mean \pm SEM) detected by HPLC within the receptor fluid over a 24 h time period after a range of skin pre-treatments (0.5mM, n=19; 1mM, n=24; 10mM, n=24) and control (0.9% NaCl, n=15); (b) concentration of CHG (mean \pm SEM) within the epidermis at 24 h after a range of skin pre-treatments; (c) concentration of CHG (mean \pm SEM) absorbed within the receptor fluid at 24 h after various skin pre-treatments.

The total concentration of CHG (as mean \pm SEM) detected within the receptor fluid at 24 h for a range of PAMAM dendrimer pre-treatments is shown in Figure 1 (c). The data was normally distributed and a Kruskal Wallis ANOVA with a Dunn's post-test confirmed that for all three concentrations of G3-PAMAM-NH₂ dendrimer skin pre-treatment tested, the total concentrations of CHG absorbed within the receptor fluids at 24 h were significantly different ($p < 0.0001$) from the physiological saline pre-treated skin (Figure 1 (c)). No significant difference in the absorption of CHG at 24 h was observed between the different PAMAM dendrimer concentrations tested ($p > 0.05$).

Franz diffusion cell studies using tape stripping to profile CHG within porcine dermatomed skin

Tape stripping studies were carried out for the 1.0 mM G3-PAMAM pre-treatment solution. A number of observations during this procedure are worthy of note as they contextualise the findings of an established method. Approximately following the 6th tape strip the skin became very moist, suggesting the removal of interstitial fluid as well as *stratum corneum* on the tape strips which was therefore recorded within the mass data [32]. The moisture attributed to interstitial fluid also caused the epidermis to tear during the tape stripping process, typically after the template had been placed over the dose area and pressure applied to the tape strip. Due to the tearing of the epidermis 21 tape strips were not obtained from each experiment. Details of the number of tape strips that were successfully removed are presented in the annotations associated with Table 3 and Figure 2 where relevant.

Table 3. Compartmental diffusion cell data of CHG concentration for control skin sample pre-treatment (n=21), vehicle control skin pre-treatment (n= 4) and 1 mM G3-PAMAM-NH₂ dendrimer skin pre-treatment (n=18).

Sample	CHG concentration following a control	CHG concentration following a vehicle control	CHG concentration following a G3-PAMAM-NH ₂ dendrimer
--------	---------------------------------------	---	--

	skin pre-treatment (n = 21)				skin pre-treatment (n = 4)				(1 mM) skin pre-treatment (n = 18)			
	CHG ($\mu\text{g}/\text{cm}^2$)		% of applied dose		CHG ($\mu\text{g}/\text{cm}^2$)		% of applied dose		CHG ($\mu\text{g}/\text{cm}^2$)		% of applied dose	
	Mean	SEM	Mean	SEM	Mean	SEM	Mean	SEM	Mean	SEM	Mean	SEM
Donor chamber	434.410	85.970	5.517	1.092	495.603	166.610	6.294	2.116	460.305	86.630	5.846	1.100
Skin wash	4416.089	516.504	56.085	6.560	3812.012	204.405	48.413	2.595	3142.011	401.605	39.904	5.100
Tape strips	1298.033	259.400	16.485	3.294	1483.080	540.783	18.835	6.868	2043.095	421.683	25.947	5.355
Epidermis / dermis	503.100	92.854	6.390	1.180	716.700	166.350	9.102	2.113	1077.502	148.991	13.684	1.892
Receptor fluid	0.017	0.017	0.0002	0.0002	0.670	0.355	0.009	0.005	0.937	0.205	0.012	0.002
Total recovered	6651.649	954.745	84.472	12.126	6508.065	1078.503	82.653	13.697	6723.850	1059.114	85.393	13.449

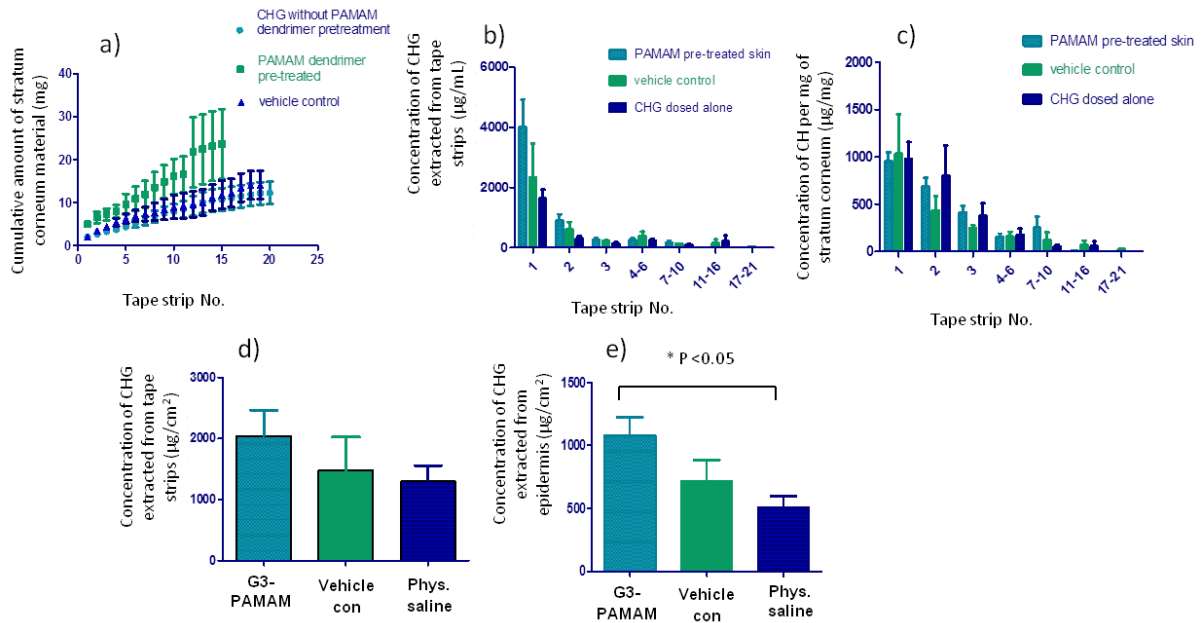


Figure 2. Figure 2. Tape stripping experiments from diffusion cell studies: (a) graph illustrating the cumulative mass of SC material on individual tape strips for various skin pre-treatments. Cumulative mass (\pm SEM) of SC material (mg) as a function of tape strip number. For CHG dosed alone $n=21$, For PAMAM dosed $n= 13$ and for vehicle control $n=3$; (b) concentration profile of CHG detected on each tape strip;(c) concentration (presented as mean \pm SEM) of CHG per mg of SC material weighed gravimetrically ($\mu\text{g}/\text{mg}$) after stripping dermatomed skin following a pre-treatment for 24 h with a 1 mM PAMAM solution of G3-PAMAM-NH₂ dendrimer ($n=13$), vehicle control ($n=3$) and CHG dosed alone ($n=21$). (d) data showing the total CHG (mean \pm SEM) extracted from the tape strips ($\mu\text{g}/\text{cm}^2$) for each of the dermatomed skin pre-dose treatments; (e) the mean total concentration ($\mu\text{g}/\text{cm}^2$) of CHG extracted from the remaining epidermis and dermis after the SC had been removed by tape stripping. A non-parametric Kruskal-Wallis test was conducted with a Dunn's post-test.

Figure 2(a) shows the mean cumulative mass of *stratum corneum* material as a function of tape strip number. This shows that similar amounts of material were collected from the pre-treatment control skin samples (solvent only as pre-treatment; 12.240 ± 2.621 mg at tape strip 20, cumulative) than for the G3-PAMAM pre-treated control sites (solvent-PAMAM solution, no CHG; 14.078 ± 3.268 mg at tape strip 19). The highest mass of *stratum corneum* material was collected from samples pre-treated with PAMAM dendrimer and then with CHG (2% w/w solution; 23.643 ± 8.113 mg at tape number 15, cumulative). It was also noted that fewer tape strips were consistently taken from the PAMAM dendrimer pre-treated skin as they were prone to being torn during the sample collection procedure.

Figure 2(b) shows the profile of CHG found in the tape strips for example the superficial layers of the *stratum corneum* (tape strips 1-3) exhibited the highest concentration of CHG and lower concentrations of CHG were found as depth into the skin increased. The PAMAM dendrimer pre-treated skin exhibited the highest amount of CHG. For example, for tape strips 7-10 the mean concentration of CHG extracted from the tape strips was $179.182 \pm 63.057 \mu\text{g/mL}$, $132.020 \pm 6.353 \mu\text{g/mL}$ and $99.874 \pm 23.293 \mu\text{g/mL}$ for PAMAM dendrimer pre-treated, vehicle control and physiological saline pre-treated skin samples, respectively. This is a 20-fold decrease in CHG concentration when compared to tape strip 1, but is still considered as a high biocidal concentration. Tape strips 7-10 showed a similar trend to tape strip 1 in that the PAMAM dendrimer pre-treated skin demonstrated the highest concentration of CHG. Due to the inconsistent nature of deeper tape strip collection, meaningful comparisons between the CHG concentrations at the higher tape strip numbers were not feasible due to the low sample number of the higher tape strips which was a result of tearing of the epidermis. Accounting for gravimetric adjustments (Equation 1), Figure 2(c) shows the concentration of CHG per mg of *stratum corneum* material removed onto the tape strips. This profile is substantially different from Figure 2(b), appearing less regular, and is most likely due to the issue of moisture associated with collecting the tape strips, usually from tape strip number 6 onwards.

Table 3 presents the mean absorption and distribution of CHG within the skin following a pre-treatment of physiological saline. Approximately 5.5% of the dosed CHG was extracted from the glass donor chamber, which is comparable to the data presented in Table 1. A total recovery of ~85% was achieved, which is an increase of ~10% when compared to the epidermal study, and is due to an increased recovery of CHG from the skin due to extraction of CHG using tape strips from the *stratum corneum*. Similarly, absorption and distribution of CHG following pre-treatment without the PAMAM dendrimer is also shown in Table 3. A similar recovery profile to earlier experiments (Table 1) was found, as is the recovery of CHG within the skin wash. The mean percentage of applied dose recovered from the tape strips, which are assumed to have removed the entire *stratum corneum*, was 1483.080

$\pm 540.783 \mu\text{g}/\text{cm}^2$. The total mean concentration of CHG recovered from the tape strips, epidermis/dermis, and receptor fluid for the vehicle control was $2200.45 \pm 707.488 \mu\text{g}/\text{cm}^2$, which is higher than the physiological saline but not significantly different ($p>0.05$).

The percutaneous absorption and distribution for CHG permeation with 1 mM G3-PAMAM-NH₂ dendrimer solution pre-treatment are shown in Table 3. There was an increase in the percentage of applied dose of CHG extracted from the tape strips, and the *stratum corneum*, when compared to the physiological saline and vehicle control experiments. The mean percentage of applied dose recovered from the tape strips was $2043.095 \pm 421.683 \mu\text{g}/\text{cm}^2$, which is the highest concentration of CHG recovered from the *stratum corneum* within the skin dermatome studies. The mean concentration of CHG absorbed within the tape strips, remaining epidermis/dermis and CHG recovered from receptor fluid was $3.12 \pm 0.57 \text{ mg}/\text{cm}^2$. Total mean recovery of CHG for this experiment was ~85%.

When the skin was pre-treated with a 1 mM solution of G3-PAMAM-NH₂ a higher concentration of CHG was extracted from the total number of tape strips, which is assumed to represent the *stratum corneum*. An increased mean CHG concentration of $2.04 \pm 0.42 \text{ mg}/\text{cm}^2$ was extracted from the tape strips following a PAMAM dendrimer pre-treatment, compared to the lower concentrations of $1.48 \pm 0.54 \text{ mg}/\text{cm}^2$ following a vehicle solution pre-treatment and $1.30 \pm 0.26 \mu\text{g}/\text{cm}^2$ was the mean CHG total extracted from all tape strips for physiological saline skin pre-treatment (Figure 2(d)). The PAMAM dendrimer pre-treatment yielded the highest concentration of CHG from the total number of tape strips compared to the treatment groups without the presence of the PAMAM dendrimer. This perceived enhancement effect is not statistically significant due to the high inherent variability observed within this study. Furthermore, Figure 2(e) shows the mean concentration of CHG within the remaining epidermal and dermal tissue following tape stripping. The CHG concentration within the epidermis and dermis shows the same trend of G3-PAMAM-NH₂>vehicle control>negative control pre-treated as that shown in Figure 2(d). After PAMAM dendrimer pre-treatment the concentration of

CHG within the skin was significantly higher than that of the skin pre-treated with physiological saline. No statistical difference was observed between the vehicle control and the negative physiological saline control ($p>0.05$).

ToF-SIMS analysis of chlorhexidine digluconate treated porcine skin cryo-sections.

A series of cryosectioned skin that included pre-treated with G3-PAMAM-NH₂ or an untreated control followed by CHG application were analysed using ToF-SIMS. The identification of a characteristic series of ion species, as reported in previous studies, [9, 16] were found which were attributed to CHG, including Cl⁻, C₇H₄N₂Cl⁻ and M-H⁻. The embedding material for cryo-sectioning, OCT, was also analysed in parallel as a reference material and there was no peak overlap. Although several ions were found which were indicative of CHG, the C₇H₄N₂Cl⁻ ion will be used exclusively as it has both relatively high chemical specificity and ion intensity enabling chemical imaging. The secondary ion images of the skin samples pre-treated with the PAMAM dendrimer show a significant increase in ion intensity throughout the skin strata for the CHG marker, C₇H₄N₂Cl⁻, compared to CHG dosed without a dendrimer pre-treatment (Figure 3(a)). The mean permeation distance of CHG into the skin, as measured by the intensity of the C₇H₄N₂Cl⁻ signal observed in Figure 3(a), was found to be 32.22 ± 1.41 μm and 47.56 ± 3.98 μm for PAMAM dendrimer untreated and PAMAM dendrimer pre-treated skin respectively. A comparison of this skin ingress is shown in Figure 3(b), which shows a significantly greater depth penetration by CHG into the skin following a pre-treatment with the PAMAM dendrimer (T test; $t=4.07$; $p<0.001$).

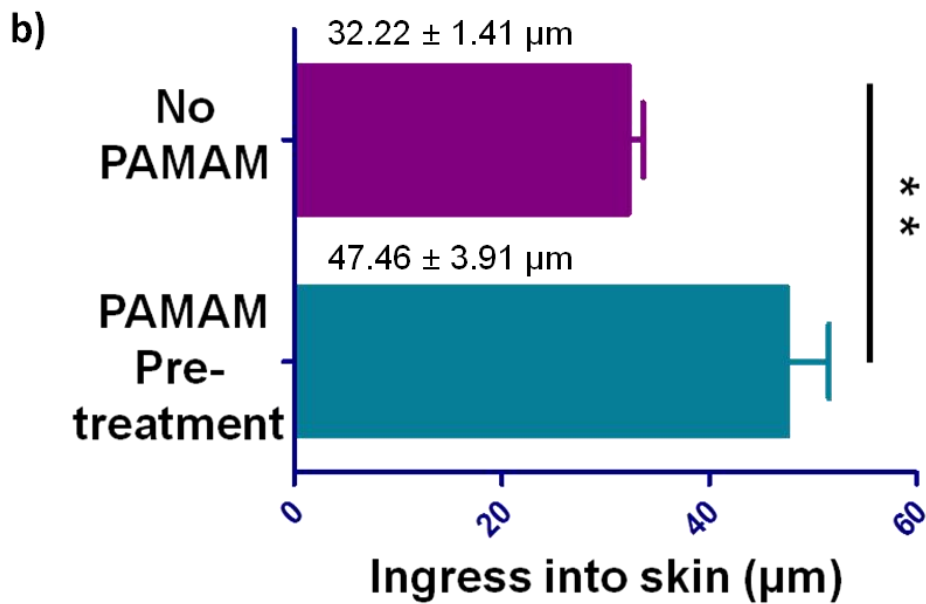
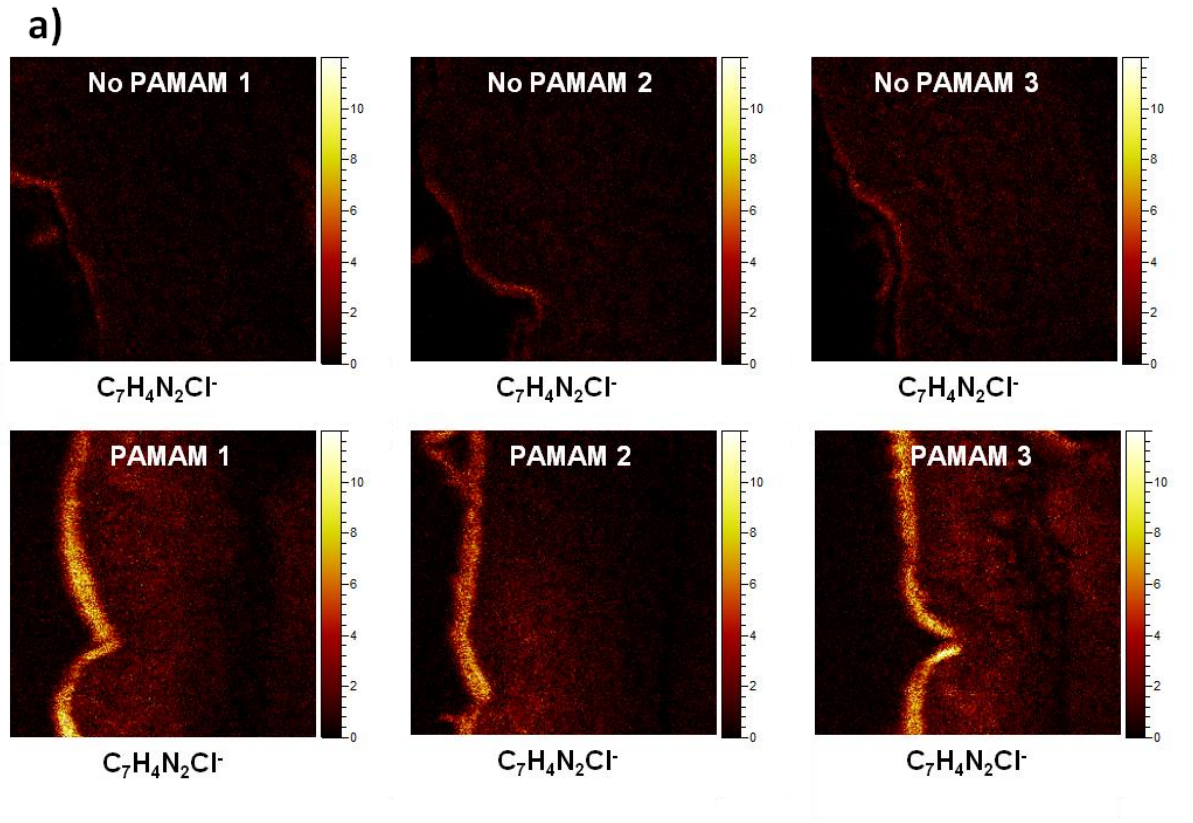


Figure 3(a). Secondary ion images of $C_7H_4N_2Cl^-$ for a pre-treatment of G3-PAMAM-NH₂ (10 mM, 0.2 mL dose) followed by an application of 2 % CHG (w/v) as compared to no PAMAM pre-treatment onto porcine dermatomed skin (400 μm thick). Field of view is 500 \times 500 μm (b) Data showing the depth permeated by CHG (2 % w/v) with and without a G3-PAMAM-NH₂ (10 mM, 0.2 mL) pre-treatment as measured using line profiles generated from the data shown in Figure 3(a).

ToF-SIMS analysis of CHG distribution on tape strips from PAMAM dendrimer pre-treated porcine skin

ToF-SIMS was previously used both for the analysis of tape stripped samples as well as cryomicrotomed cross-sections whereby the observation of CHG in both acted as a cross-validation of the methods used for the analysis of CHG within porcine skin [9, 16]. Figure 4 shows the secondary ion images of $C_7H_4N_2Cl^-$ for individual tape strips analysed by the ToF-SIMS. An even distribution of CHG can be observed across each tape strip up until tape strip 14 where it then becomes more heterogeneous (Figure 4). The application of CHG alone demonstrates the decrease in CHG with increasing tape strip number (representing an increase in depth) removed. There is also a decrease in the amount of stratum corneum removed with increasing tape strip number (Figure 4). The secondary ion intensity data produced by the ToF-SIMS analysis of the tape strips were used to observe the enhanced distribution and permeation of CHG following a G3-PAMAM-NH₂ pre-dose treatment (Figure 5)). The skin pre-treated with the PAMAM dendrimer exhibited a greater intensity of the CHG marker across the upper skin strata, with $C_7H_4N_2Cl^-$ being observed throughout the *stratum corneum* (Figure 5). Figure 5 demonstrates that permeation of CHG following dendrimer pre-treatment is significantly greater, and that CHG penetrates into the *stratum corneum*, compared to permeation in the absence of a dendrimer pre-treatment. Without a PAMAM dendrimer pre-treatment the CHG signal decreases markedly at tape strip 13 however after a PAMAM dendrimer pretreatment the CHG signal is still strong showing elevated CHG concentrations in the deeper layers of the *stratum corneum*.

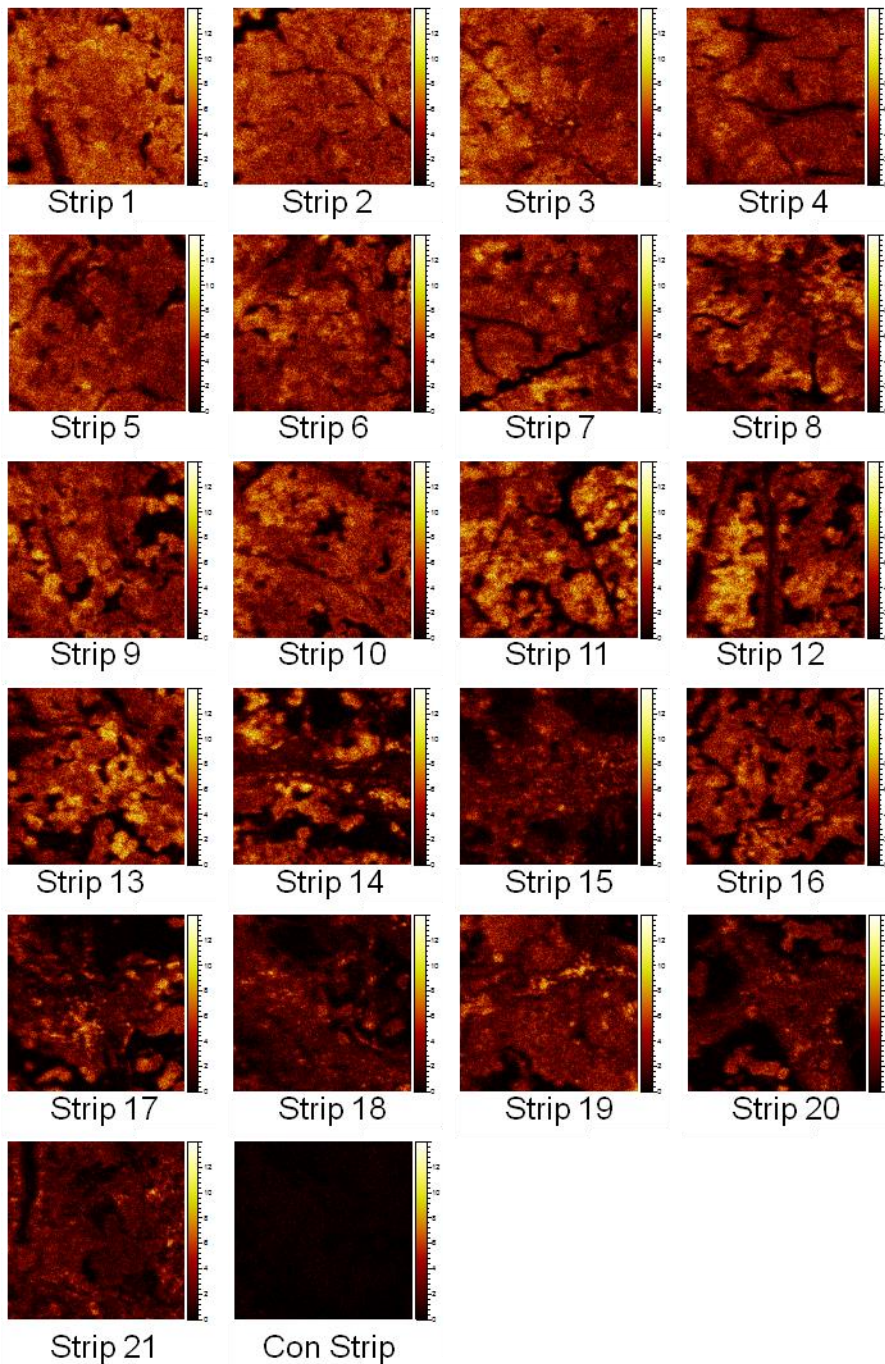


Figure 4. ToF-SIMS secondary ion images of $C_7H_4N_2Cl^-$ for 21 consecutive tape strips taken from 2% CHG (w/v) dosed porcine dermatomed skin (400 μm thick) and two tape strips taken from an untreated control, field of view 500 x 500 μm . Image adapted from [16].

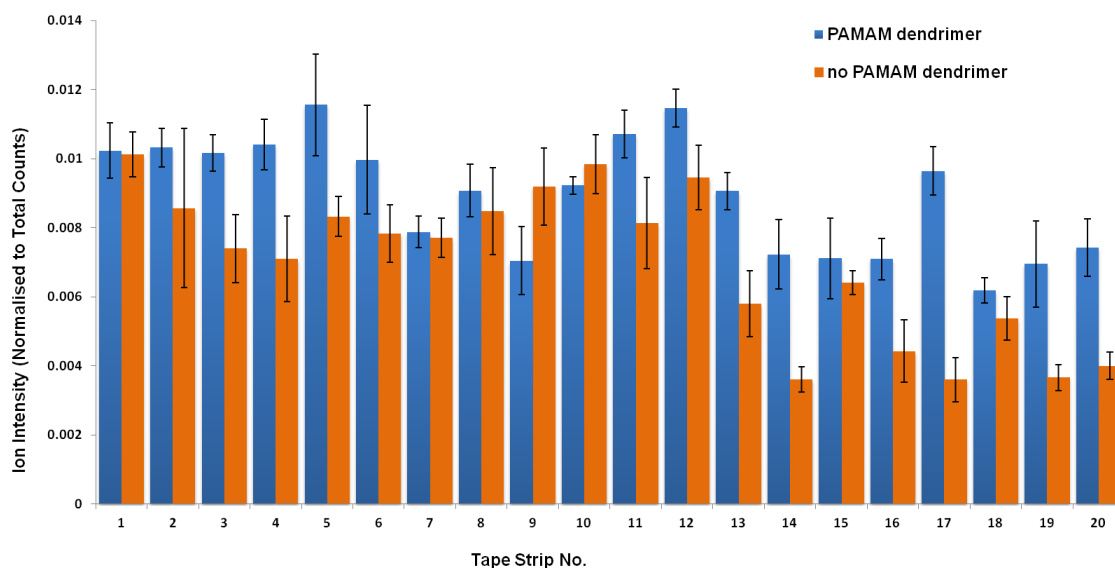


Figure 5. $C_7H_4N_2Cl^-$ ion intensity assigned to CHG, for 20 consecutive tape strips taken from CHG dosed alone (2 % w/v) to porcine skin ($n=4 \pm SD$) and to G3-PAMAM-NH₂ (10 mM, 0.2 mL dose, 24 h) pre-treated porcine skin then dosed with CHG dosed (2 % w/v) ($n=4 \pm SD$).

DISCUSSION

Penetration enhancement effect of G3-PAMAM-NH₂ analysed by HPLC

The results of the Franz cell studies clearly indicate that the skin permeation of CHG increased by up to 30-fold, when preceded by a PAMAM dendrimer pre-treatment (Table 2). Enhancement was not concentration dependent but showed a similar effect over the concentration range examined in this study, relative to control (Figures 1 (b) and (c)). The lack of a clearly defined dose-response in this case is most likely due to the high variability observed in the diffusion cell studies, which might be partly attributed to inherent variation associated with such experimental protocols, but also to the recovery of CHG (Table 1) which, was often variable. This would likely be due to the number of cationic amine groups on the CHG able to bind to tissue and glassware and this may have influenced the statistical significance of the outcome. Nevertheless, the results obtained herein clearly demonstrate that the pre-treatment of skin with the PAMAM dendrimer significantly increases skin permeation of CHG observed in *in vitro* diffusion cell studies. A similar effect has been reported previously for 5-fluorouracil following pre-treatment of the skin with a G4-PAMAM-NH₂ dendrimer [26]. In this study

the proposed mechanism of action / enhancement was to the interaction of cationic dendrimers with the skin lipid bilayers, where reductions of skin resistance were observed with a range of dendrimer molecules, suggesting that the dendrimers chemically altered the composition of skin lipid bilayers. Other studies have shown a 4-fold increase in the skin permeation of tamsulosin hydrochloride following dendrimer pre-treatment [21]. The authors also reported that a similar enhancement was not observed for two other drugs, namely ketoprofen and clonidine, and suggested that the electrostatic interaction between the drug and the dendrimer was key to its enhancement effect. In addition, it was also suggested that these enhancement effects have been attributed to dendrimer aggregation at high concentrations [35].

The exact mechanism of enhanced topical and transdermal drug delivery by dendrimers is still unknown but is suggested to be attributed to action as a drug release modifier thereby increasing drug dissolution, preferential accumulation within the appendages of the skin and impairing the barrier function of the *stratum corneum* [23]. PAMAM dendrimers have been suggested as a drug release modifier with a cyclodextrin-like mechanism in that they can act as a carrier system for the lipophilic drug indomethacin (log P 4.3) [21]. As with PAMAM dendrimers, lipophilic drugs form an electrostatic or hydrophobic complex with cyclodextrins that then increases the solubility of a drug within an aqueous vehicle. This then results in an increase in the concentration of drug that can partition into the *stratum corneum* [36].

This is the first study to investigate PAMAM dendrimers as a topical penetration enhancer of an antiseptic with the aim of increasing the exposure of the bacteria in skin to the CHG. Pre-treatment of the skin with G3-PAMAM (0.5 – 10.0 mM) resulted in an increase not only to the rate of CHG skin permeation, but also caused a significant decrease in its lag time to achieve steady-state permeation much quicker when compared to CHG permeation without PAMAM pre-treatment as shown in Table 2. It is therefore reasonable to comment that PAMAM dendrimer facilitated skin absorption would

result in a much faster and hence more effective action. An efficacious antiseptic has been described by the Food and Drug Administration (FDA) for healthcare antiseptic drug products as “a fast-acting [rapidly kills microorganisms], broad spectrum [kills a wide variety of microorganism species], persistent [suppresses regrowth of remaining microorganisms], antiseptic containing preparation that significantly reduces the number of microorganisms on intact skin” [38]. However, while it is clear that CHG possesses these attributes the compound poorly penetrates the skin. Thus, the application of PAMAM dendrimers to topically applied systems may reduce the lag time and better facilitate the antiseptics of the deeper skin layers, as greater permeation would occur within a shorter time frame. Such a capability therefore addresses the first requirement of the FDA monograph “more effectively”, potentially offering increased efficacy of the antibacterial agent when it is applied to the skin with a dendrimer.

It was observed throughout the diffusion cell experiments that, once the vehicle had evaporated (*ca.* 3-6 h), a viscous and adhesive layer of G3-PAMAM-NH₂ dendrimer was deposited across the skin surface. This has been attributed to the highly hygroscopic nature of PAMAM dendrimers [17] that extract water from the surrounding environment to exist in a gel-like state. Thus, a dense PAMAM dendrimer layer distributed across the skin surface may reduce the TEWL from the skin, causing skin hydration and thereby acting as a possible mechanism of enhancement for the skin permeation of CHG. Occlusion of the skin leading to increased hydration has been a known mechanism of skin penetration for certain compounds for many years [38, 39]. The water content of the *stratum corneum* is typically 15-20% (dry weight) but can increase up to 400% of the dry weight of tissue under occlusion and increased humidity [40]. Occlusion has been utilised as a permeation enhancer for a range of therapeutics and biomolecules, most commonly in transdermal skin patches, but also in other systems, including fluorescein isothiocyanate-bovine serum albumin [41] and ¹⁴C acetylsalicylic acid [42]. On hydration of the skin, corneocytes of the *stratum corneum* become highly swollen increasing the cell volume [43]. Hydrating the skin for permeation enhancement of a wide range of therapeutics

has been used for many years, but it does not enhance the skin permeation of all compounds [44, 45]. Hence other mechanisms for improving drug delivery across the skin – such as we have presented here – provide an alternative strategy.

There was an increase in CHG concentration within the epidermis and dermis when the PAMAM pre-treated skin was compared to the physiological saline pre-treated skin for in vitro diffusion cell studies (Figure 1 (b) and (c)). These results indicate that the PAMAM dendrimer pre-treatment increases the deposition of CHG within not only the superficial layers of the *stratum corneum* but also the epidermis and dermis. The aim of this study was to increase the penetration and retention of CHG within the skin and this has been demonstrated within the epidermis and percutaneous absorption studies presented herein. An increase in the deposition of CHG within the skin may therefore improve antibacterial efficacy by increasing the exposure of opportunistic pathogens to CHG [2].

In addition to the improvement in limit of detection offered by ToF-SIMS, compared to HPLC-facilitated tape stripping the ToF-SIMS method is able to provide additional information on the permeation process. For example, one additional important consideration is that the ToF-SIMS method provides evidence of the uniformity of delivery into the skin, something that is complementary *and* additional to the tape-stripping studies. It demonstrates that chlorhexidine is not penetrating via specific channels, such as skin appendages or via small, localised areas and that permeation is moving uniformly through the skin. The cross-sectioned data also allows a visualisation of permeation that could allow a correlation with the different physiological layers in the skin in greater detail.

For example, Figure 7 shows that, in term of physiological correlation, PO is well known to be more prevalent in the epidermis than the *stratum corneum*. The PO_2^- image thus denotes the end of the *stratum corneum* and so allows this strata to be accurately observed. It also shows that this strata contains a substantial amount of chlorhexidine and that significantly less chlorhexidine is present in the deeper skin tissues.

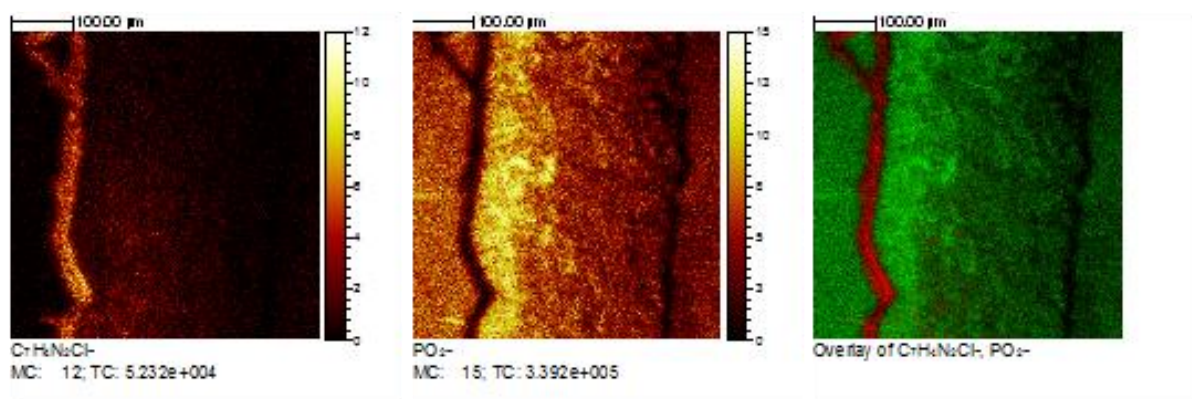


Figure 7. Co-localisation of chlorhexidine in the skin with skin structures, identified by the presence of PO₂⁻ fragments, which are normally localised to the *stratum corneum*.

Penetration enhancement effect of G3-PAMAM-NH₂ analysed by ToF-SIMS

Despite issues with the variation of tissue and the complexities of fully characterising the skin permeation of exogenous chemicals, correct use of the OECD 428 *in vitro* Franz diffusion cell approach provides a good surrogate for dermal absorption in man. This study supports the previously reported use of the ToF-SIMS technique in characterising the actual chemistry in skin during the absorption process. This is not, of course, a replacement for diffusion cell studies but it is certainly a valuable complementary technique which allows visualisation of a permeant within the skin cross-sections, allows the acquisition of real permeation depth values including those which are relevant, when compared to histological samples, to skin structural features and which provides a semi-quantitative assessment of permeation into skin.

Skin diffusion cell experiments in this study have shown that pre-treatment of the skin with dendrimers significantly enhanced CHG absorption. This is clearly supported by the ToF-SIMS experiments, where the permeation enhancement could also be visualised (Figure 3). While CHG could be readily detected by the ToF-SIMS through unique fragment identification, those fragment ions detected that correspond to the dendrimer were not sufficiently unique to be distinguished from the

endogenous skin components. This is due to G3-PAMAM dendrimers being constituted of polymeric branches of amides and carboxyl groups which appear in the skin in abundance. As such no comment on the skin permeation of G3-PAMAM dendrimers can be made. However, a clear intensity increase of the CHG markers within the upper skin strata was observed which was attributed to the penetration enhancement effect of the PAMAM dendrimer. When the PAMAM dendrimer-treated skin is compared to the skin treated with CHG alone, the considerable penetration and deposition enhancement is clearly evident. We have also showed a significant ($t=4.07$, $p<0.001$) penetration depth increase of CHG following PAMAM pre-treatment which indicates that permeation had progressed approximately 15 μm further into the skin compared to CHG delivery in the absence of PAMAM enhancement.

CONCLUSIONS

The results of this study indicate that a pre-treatment of the skin with G3-PAMAM dendrimers significantly increases the amount and depth of permeation of CHG into porcine skin *in vitro*. This observation could be of great significance in terms of the efficiency and effectiveness of antibacterial treatment and may potentially be extrapolated to other topical products. While the mechanism for enhanced dermal delivery is still unclear, requiring further investigation, it is proposed that the PAMAM dendrimer enhances dermal absorption either by barrier lipid disruption or by occluding the skin surface. The *ex vivo* diffusion cell experiments in pig skin have been complimented by the ToF-SIMS method, specifically adding the visualisation of the drug in the skin layers. This allows the potential for mapping the co-localisation of specific permeants with skin structures (i.e. the proximity of permeants to skin layers, such as the *stratum corneum*) thus providing a greater ability to characterise penetration enhancers, drug delivery systems, skin absorption and to understand the mechanism of permeation. The sensitivity of the technique also allows for a more accurate depth profile of CHG permeation within the skin to be obtained.

REFERENCES

1. G.W. Denton, Chlorhexidine, in: S.S. Block (ed.), Disinfection, sterilization and preservation, 4th edn., Lea and Febiger, Philadelphia, 1991, pp. 274-289.
2. T.J. Karpanen, T. Worthington, B.R. Conway, A.C. Hilton, T.S.J. Elliott, P.A. Lambert, Penetration of chlorhexidine into human skin, *Antimicrob. Agents Chemother.*, 52 (2008) 2633-3636.
3. C. Lafforgue, L. Carret, F. Falson, M. Reverdy, J. Freney, Percutaneous absorption of a chlorhexidine digluconate solution, *Int. J. Pharm.*, 147 (1997) 243-246.
4. R.G. van der Molen, F. Spies, J.M. vant Noordende, E. Boelsma, A.M. Mommaas, H.K. Koerten, Tape stripping of human stratum corneum yields cell layers that originate from various depths because of furrows in the skin, *Arch. Dermatol. Res.*, 289 (1997) 514-518.
5. E. Marttin, M.T.A. Neelissen-Subnel, F.H.N Dehaan, H.E. Bodde, A critical comparison of methods to quantify stratum corneum removed by tape stripping, *Skin Pharmacol.*, 9 (1996) 69-77.
6. C.S. King, S. Barton, S. Nicholls, R. Marks, Changes in properties of the stratum corneum as a function of depth, *Br. J. Dermatol.*, 100 (1979) 165-172.
7. Y.N. Kalia, F. Pirot, R.H. Guy, Homogenous transport in a heterogeneous membrane: Water diffusion across human stratum corneum in vivo, *Biophys. J.*, 71 (1996) 2692-2700.
8. K.L. Trebilcock, J.R. Heylings, M.F. Wilks, In-vitro tape stripping as a model for in-vivo skin stripping, *Tox. In Vitro*, 8 (1994) 665-667.
9. A.M. Judd, D. Scurr, J. Heylings, K.-W. Wan, G.P. Moss, Development of Time-of-Flight Secondary Ion Mass Spectrometry in evaluating tissue-specific percutaneous absorption, in: K.R. Brain, R. Chilcott (eds.), *Advances in the Dermatological Sciences*, Royal Society of Chemistry, Cambridge, 2013, pp. 340-354.
10. J. Vickerman, ToF-SIMS – Surface analysis by mass spectrometry, in J. Vickerman, D. Briggs (eds.), *Surface analysis by mass spectrometry*, 2nd edn., IMP Publications, Chichester, 2001.
11. A. Benninghoven, Chemical analysis of inorganic and organic surfaces and thin films by static Time-of-Flight Secondary Ion Mass Spectrometry (ToF-SIMS), *Angewandte Chemie – International Edition in English*, 33 (1994) 1023-1043.
12. T.G. Lee, J.-W. Park, H.K. Shon, D.W. Moon, K. Li, J.H. Chung, Biochemical imaging of tissues by SIMS for biomedical applications, *App. Surf. Sci.*, 255 (2008) 1241-1248.
13. M. Okamoto, N. Tanji, Y. Katayama, J. Okada, ToF-SIMS investigation of the distribution of a cosmetic agent in the epidermis of the skin., *App. Surf. Sci.*, 252 (2006) 6805-6808.
14. N. Tanji, M. Okamoto, Y. Katayama, M. Hosokawa, N. Takahata, Y. Sano, Investigation of the cosmetic ingredient distribution in the stratum corneum using NanoSIMS imaging, *App. Surf. Sci.*, 255 (2008) 1116-1118.

15. N.J. Starr, D.J. Johnson, J. Wibawa, I. Marlow, M. Bell, D.A. Barrett, D.J. Scurr, Age-related changes to human stratum corneum lipids using Time-of-Flight Secondary Ion Mass Spectrometry following in vivo sampling, *Anal. Chem.*, 88 (2016) 4400-4408.
16. A.M. Judd, D. Scurr, J. Heylings, K.-W. Wan, G.P. Moss, Distribution and visualisation of chlorhexidine within the skin using ToF-SIMS. A potential platform for the design of more efficacious skin antiseptic formulations, *Pharm. Res.*, 30 (2013) 1896-1905.
17. S. Uppuluri, S.E. Keinath, D.A. Tomalia, P.R. Dvornic, Rheology of dendrimers. 1. Newtonian flow behaviour of medium and highly concentrated solutions of polyamidoamine (PAMAM) dendrimers in ethylenediamine (EDA) solvent, *Macromol.* 31 (1998) 4498-4510.
18. M.T. Morgan, Y. Nakanishi, D.J. Kroll, A.P. Griset, M.A. Carnahan, M. Wathier, N.H. Oberlies, G. Manikumar, M.C. Wani, M.W. Grinstaff, Dendrimer-encapsulated camptothecins: increased solubility, cellular uptake and cellular retention affords enhanced anticancer activity in vitro, *Cancer Res.*, 66 (2006) 11913-11921.
19. O. Milhem, C. Myles, N. McKeown, D. Attwood, A. D'Emanuele, Polyamidoamine Starburst® dendrimers as solubility enhancers, *Int. J. Pharm.* 197 (2000) 239-241.
20. U. Gupta, H.B. Agashe, A. Asthana, N. Jain, Dendrimers: novel polymeric nanoarchitectures for solubility enhancement, *Biomacromol.* 7 (2006) 649-658.
21. B. Wang, R.S. Navath, A.R. Menjoge, B. Balakrishnan, R. Bellair, H. Dai, R. Romero, S. Kannan, R.M. Kannan, Inhibition of bacterial growth and intramniotic infection in a guinea pig model of chorioamnionitis using PAMAM dendrimers, *Int. J. Pharm.*, 395 (2010) 298-308.
22. Y. Cheng, Q. Wu, Y. Li, T. Xu, External electrostatic interaction versus internal encapsulation between cationic dendrimers and negatively charged drugs: which contributes more to solubility enhancement of drugs, *J. Phys. Chem. B*, 112 (2008) 8884-8890.
23. M. Sun, A. Fan, Z. Wang, Y. Zhao, Dendrimer-mediated drug delivery to the skin, *Soft Matter*, 8 (2012) 4301-4305.
24. Y. Zhao, X. Fan, D. Liu, Z. Wang, PEGylated thermo-sensitive poly(amidoamine) dendritic drug delivery systems, *Int. J. Pharm.*, 409 (2011) 229-236.
25. J.M. Criscione, B.L. Le, E. Stern, M. Brennan, C. Rahner, X. Papademetrix, T.M. Fahmy, Self-assembly of pH-responsive fluorinated dendrimer-based particulates for drug delivery and non-invasive imaging, *Biomaterials*, 30 (2009) 3946-3955.
26. V.V.K. Venuganti, O.P. Perumal, Effect of poly(amidoamine) (PAMAM) dendrimer on skin permeation of 5-fluorouracil, *Int. J. Pharm*, 361 (2008) 230-238.
27. A.S. Chauhan, A.S., S. Svidevi, K.B. Chalasani, A.K. Jain, S.K. Jain, N. Jain, P.V. Diwan, Dendrimer-mediated transdermal delivery: enhanced bioavailability of indomethacin, *J. Cont. Rel.*, 90 (2003) 335-343.
28. A. Bhatti, R. Scott, A. Dyer, In vitro percutaneous absorption: pig epidermal membrane as a model for human skin, *J. Pharm. Pharmacol.*, 40 (Suppl.) (1988) pp. 45.

29. I.P. Dick, R.C. Scott, Pig ear as an in vitro model for human skin permeability, *J. Pharm. Pharmacol.*, 44 (1992) 640-645.
30. R.C. Scott, H.M. Clowes, In vitro percutaneous absorption experiments: a guide to the technique for use in toxicology assessments, *Tox. Mech. Meth.*, 2 (1992) 113-123.
31. D. Davies, R. Ward, J. Heylings, Multi-species assessment of electrical resistance as a skin integrity marker for in vitro percutaneous absorption studies, *Tox. In Vitro*, 18 (2004) 351-358.
32. J. Lademann, U. Jacobi, C. Surber, H.J. Weigmann, J.W. Fluhr, The tape stripping procedure – evaluation of some critical parameters, *Eur. J. Pharm. Biopharm.*, 72 (2009) 317-323.
33. M.B. Reddy, A.L. Stinchcomb, R.H. Guy, A.L. Bunge, Determining dermal absorption parameters in vivo from tape strip data, *Pharm. Res.* 19 (2002) 292-298.
34. F. Pirot, Y.N. Kalia, A.L. Stinchcomb, G. Keating, A. Bunge, R.H. Guy, Characterization of the permeability barrier of human skin in vivo, *Proc. Nat. Acad. Sci.*, 94 (1997) 1562-1567.
35. B. Klajnert, R. Epan, PAMAM dendrimers and model membranes: Differential scanning calorimetry studies, *Int. J. Pharm.*, 305 (2005) 154-166.
36. J. Legendre, I. Rault, A. Petit, W. Luijten, I. Demuyck, S. Horvath, Y. Ginot, A. Cuine, Effects of β -cyclodextrins on skin: implications for the transdermal delivery of pirobedil and a novel cognition-enhancing drug, S-9977, *Eur. J. Pharm. Sci.*, 3 (1995) 311-322.
37. Federal Register, Topical antimicrobial drug products for over-the-counter human use: tentative final monograph for health-care antiseptic drug products, 59 (1994) 31402-31452 (21 CFR Parts 333 and 369), US Food And Drug Administration.
38. M. Roberts, M. Walker, Water. The most natural penetration enhancer, *Drugs Pharm. Sci.*, 59 (1993) 1-30.
39. R. Wester, H. Maibach, Penetration enhancement by skin hydration. *Percutaneous Penetration Enhancers*, CRC Press, Boca Raton, 1995, pp. 21-28.
40. A.C. Williams, B.W. Barry, Penetration Enhancers, *Adv. Drug Del. Rev.*, 64 (2012), 128-137.
41. G. Tan, P. Xu, L.B. Lawson, J. He, L.C. Freytag, J.D. Clements, V.T. John, Hydration effects on skin microstructure as probed by high-resolution cryo-scanning electron microscopy and mechanistic implications to enhanced transcutaneous delivery of biomacromolecules, *J. Pharm. Sci.*, 99 (2009) 730-740.
42. W.C. Fritsch, R.B. Stoughton, A. Stapelfeldt, The effect of temperature and humidity on the penetration of ^{14}C -acetylsalicylic acid in excised human skin. *J. Invest. Dermatol.* 41 (1963) 307-311.
43. J.A. Bouwstra, A. de Graaff, G.S. Gooris, J. Nijse, J.W. Wiechers and A.C. van Aelst, Water distribution and related morphology in human stratum corneum at different hydration levels. *J. Invest. Dermatol.* 120(5), (2003) 750-758.
44. D. Bucks, H.I. Maibach, 4. Occlusion does not uniformly enhance penetration in vivo. *Drugs Pharm. Sci.*, 97 (1999) 81-106.

45. L.J. Taylor, R.S. Lee, M. Long, A.V. Rawlings, J. Tubek, L. Whitehead, G.P. Moss, Effect of occlusion on the percutaneous penetration of linoleic acid and glycerol, *Int. J. Pharm.*, 249 (2002) 157-164.